Poloidal rotation asymmetry and relation to turbulence

A. Krämer-Flecken[1], Y. Xu[2], S. Zoletnik[3] and the TEXTOR team

[1] *Institut für Energie- und Klimaforschung / Plasmaphysik, Forschungszentrum Jülich GmbH, EURATOM Association, D–52425 Jülich, Germany*

[2] *Laboratoire de Physique des Plasmas, Association Euratom-Belgian state, Ecole Royale Militaire, B-1000 Brussels, Belgium*

[3] *Institute for Particle and Nuclear Physics (RMI), Association EURATOM/HAS, Budapest, Hungary*

Introduction

Recent papers report on poloidal asymmetries on turbulence properties [1]. The equilibrium but also the fluctuating plasma edge quantities as electron density, temperature and floating potential show significant differences on in and outboard side at $r/a \approx 0.9$. Measurement of turbulence spectra [2] at the edge of the confinement region and observed on outer and inner midplane as well as on the top show remarkable differences [3]. Moreover derivated turbulence properties such as radial correlation length show a dependence on the poloidal angle of the measurement. Regarding top bottom asymmetries the direction of plasma current and magnetic field show an influence on the density fluctuation level [4, 5]. All these experiments suggest that also macroscopic quantities may be influenced by the asymmetry in the turbulence properties. Indeed recent three dimensional turbulence simulations [6] could show that the intrinsic rotation depends on heat flux derived from turbulence properties. Moreover, it is shown recently that radial inhomogeneities can produce turbulence driven intrinsic rotation [7].

This paper will report on the measurements performed on TEXTOR with Correlation Reflectometry and discusses possible relations between turbulence properties and the asymmetry in rotation.

Experiment

At TEXTOR ($R_0 = 1.75\,\text{m}, a = 0.46\,\text{m}$) the existing O-mode Correlation Reflectometry (CR) system [8, 9] is used to monitor macroscopic plasma quantities like $v_\perp$ at $\theta \approx 105^\circ$ and $\theta = 0^\circ$ (low field side or LFS) of the device. In addition also turbulence properties are monitored such as decorrelation time τ_{dc} and turbulence wave length $\lambda_\perp$, simultaneously. O-mode reflectometry guarantees that the reflection layer is independent from the poloidal angle and only determined by the plasma frequency. The system consists of one antenna array on the top of the vessel and two other arrays on the outer midplane. The arrays consists of 2-4 receiving antenna. The system can be operated either on midplane or top. However, simultaneous measurements of top and midplane antennae within one discharge are possible, too. The top array is not mounted exactly at R_0 but shifted to the high field side by $s = 0.08\,\mathrm{m}$ which causes a increasing poloidal angle (θ) with decreasing reflection layer and yielding $104^\circ \leq \theta \leq 110^\circ$. Experiments reported here are performed in ohmic plasmas with the following parameters: $300\,\mathrm{kA} \leq I_p \leq 400\,\mathrm{kA}$, $1.9\,\mathrm{T} \leq B_t \leq 2.25\,\mathrm{T}$ and $2 \times 10^{19}\,\mathrm{m}^{-3} \leq n_e \leq 3 \times 10^{19}\,\mathrm{m}^{-3}$. The radial range in the experiments under investigation covers $0.72 \leq r/a \leq 0.85$. The reflection layer r_c is estimated from the 9 channel HCN interferometer at TEXTOR. Within each discharge flat top 8 different radial positions are probed. Horizontal and vertical plasma positions are kept constant during this phase. The perpendicular rotation is deduced from cross correlation analysis of the different antennae combinations and cross phase analysis.

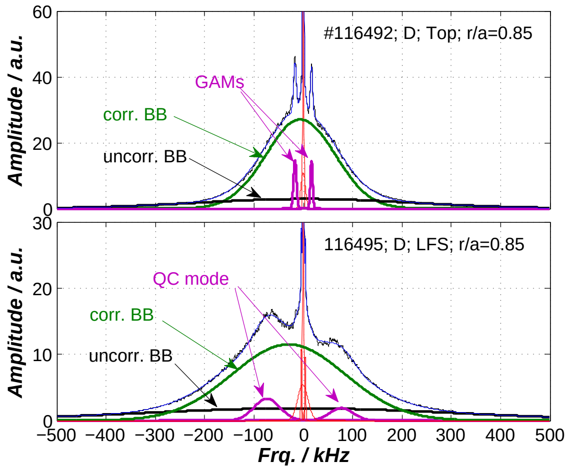

Figure 1: *Comparison between top and LFS spectrum for antennae D. Turbulence components are shown for each spectrum*

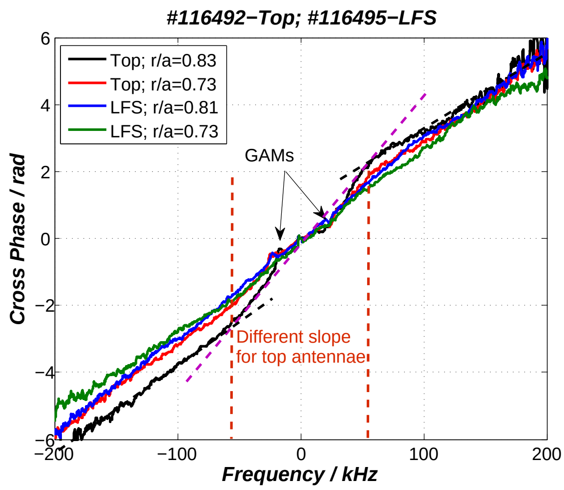

Figure 2: *Unwrapped cross phase for top and LFS array, at minimum and maximum r_c. Clearly the influence of the GAM is seen.*

Results and Discussion

The complex amplitude spectra of an antennae from the top and outer LFS are compared in fig. 1. Both spectra are measured at the $r/a = 0.85$. Both discharges have the same plasma parameters. Also the signal processing chain as mixer, quadrature detector and ADC are the same. On a first glance the spectrum on the LFS is broader than the top one. A common feature is the correlated and uncorrelated broad band (BB) turbulence. The transition from correlated to uncorrelated BB turbulence is marked by the beginning of the scatter in the cross phase between two antenna. The full width at $1/e$-level is larger at the LFS antenna for $r_c/a \geq 0.77$. In addition geodesic acoustic modes (GAMs) are seen in the spectrum of the top antennae and quasi coherent modes show up pronounced at the LFS antennae. Interesting to note is the measurement of the cross phase (Φ) between the same two antennae (D, E) separated by

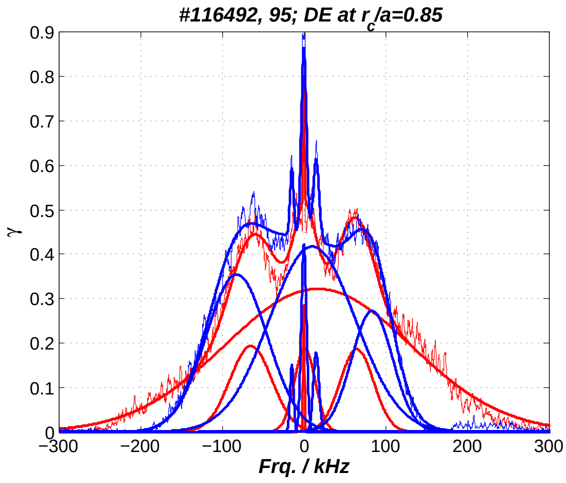

Figure 3: *Decomposition of coherence spectrum for top (blue) and LFS (green).*

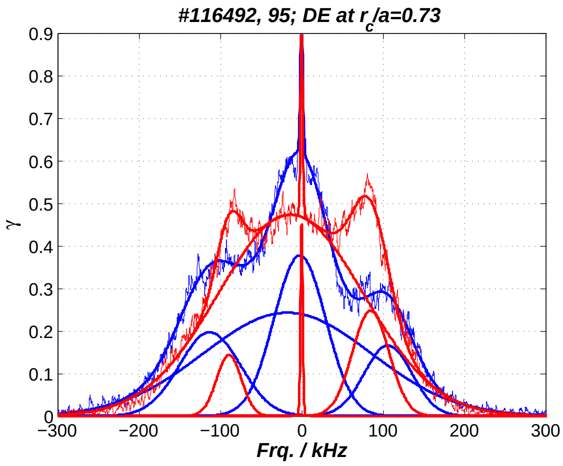

Figure 4: *Same as for fig. 3 but for different r_c/a.*

$\Delta\theta = 0.05\,\mathrm{rad}$ from top and LFS array and which is shown in fig. 2. The cross phase is a measure for the perpendicular rotation as it is defined by $\Omega_\perp = 2\pi\Delta\theta/(d\Phi/df)$, where $\Delta\theta$ denotes the poloidal angle between the two antennae and the propagation time is defined as $\Delta t = d\Phi/df/(2\pi)$. Measurements of Δt are deduced from the slope of Φ for the frequency range $(-200\,\mathrm{kHz} \le f \le 200\,\mathrm{kHz})$. At the LFS the slope does not change very much with decreasing r_c. However, for the top position different slopes can be identified in fig. 2 (see black line for $r/a = 0.83$). In the range $-60\,\mathrm{kHz} \le f \le 60\,\mathrm{kHz}$, $d\Phi/df$ is much larger compared to $|f| > 60\,\mathrm{kHz}$ where the slope becomes smaller. With decreasing r_c the difference in the slopes for the top disappears and top and LFS show similar slopes over the whole frequency range.

This evident result shows that the turbulence consists of different components with even different propagation properties. The analysis of the coherence spectra allows the decomposition into turbulence components. In fig. 3 and fig. 4 the components at fixed r_c are shown for top and LFS, for the same conditions as in fig. 2. The decomposition of the coherence spectrum is consistent with the different slopes in the cross phase spectrum. A major difference is seen for the BB turbulence in FWHM and amplitude. At $r/a = 0.85$ this component broad with an amplitude of $A = 0.34$ at the LFS. However, it is narrow with $A = 0.42$ at the top. The QC modes have a smaller amplitude on the LFS but dominating in the top spectrum. With decreasing r_c the difference between top and LFS for the BB turbulence disappears and at $r/a \approx 0.73$ they have equal width. Due to O-mode CR the measurements are performed on the same isodensity surface. The measurement show an asymmetry in $\Omega_\perp$ on isodensity surfaces. Cross correlation analysis yield $\Omega_\perp^{top} = 2.8\,\mathrm{km\,s^{-1}}$ and $\Omega_\perp^{LFS} = 4.2\,\mathrm{km\,s^{-1}}$ at the outermost position.

To investigate the a possible parametric dependence of the asymmetry a current ramp $(320\,\mathrm{kA} \le I_p \le 460\,\mathrm{kA})$ is performed during the discharge. In this shot two antennae measured at the top and two at the LFS, simultaneously. Both having $\Delta\theta = 0.075\,\mathrm{rad}$. The delay time Δt is calculated with cross correlation analysis filtered in the range $20\,\mathrm{kHz} \leq f \leq 200\,\mathrm{kHz}$. An increase of the time difference between top and LFS estimated in $50\,\mathrm{ms}$ steps is observed with decreasing I_p (see fig. 5).

Besides the information on turbulence propagation the CR system measures other turbulence properties as well. The calculation of τ_{dc} and $\lambda_\perp$ is based on poloidal evolution of the cross correlation coefficient of filtered time series according to the major components observed in the spectra at $r_c/a = 0.85$; (i) $|f| \leq 60\,\mathrm{kHz}$ for top and (ii) $60\,\mathrm{kHz} \leq |f| \leq 200\,\mathrm{kHz}$ for LFS. No significant difference in τ_{dc} is found. However, $\lambda_\perp \approx 20\,\mathrm{mm}$ on top and $\lambda_\perp \approx 86\,\mathrm{mm}$ on the LFS is measured. The estimated poloidal wave number on the LFS is with $k_\perp = 0.7\,\mathrm{cm}^{-1}$ much smaller than at the top with $k_\perp = 3.1\,\mathrm{cm}^{-1}$. From single antennae the phase fluctuation σ_Φ is measured. As usual σ_Φ increases towards the edge. On the LFS σ_Φ is a factor 1.4 higher than on the top. Together with an increased σ_Φ at the LFS level the observations support a ballooning turbulence on the LFS.

Summary

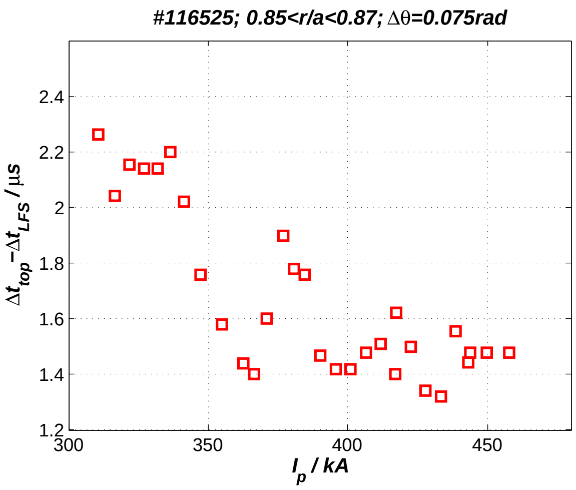

Figure 5: *Asymmetry in Δt as function of I_p increases with decreasing I_p*

At TEXTOR the perpendicular velocity $\Omega_\perp$ of the plasma is studied with CR at two poloidal positions. At outermost position $\Omega_\perp$ at the LFS is about 50% higher than on top. The asymmetry decrease towards the center and is related to the different components in the turbulence spectrum. The cross phase and coherence analysis shows that the asymmetry stems from the different slopes in the range $-60\,\mathrm{kHz} \leq f \leq 60\,\mathrm{kHz}$. The observation demonstrate that the plasma does not rotate like a rigid body and shows poloidal asymmetry. The small $k_\perp$ measured on the LFS together with increased fluctuation level supports that the turbulence on the LFS has a ballooning like structure.

References

[1] C. Silva, H. Figueiredo, P. Duarte et al., Plasma Phys. Control. Fusion **53**, 085021 (2011)
[2] V.A. Vershkov, D.A. Shelukhin, S.V. Soldatov et al., Nucl. Fusion, **45**, S203-S226 (2005)
[3] V.A. Vershkov, V.F. Andreev, A.A. Borschegovskiy et al., Nucl. Fusion, **51**, 094019 (2011)
[4] D.L. Brower, W.A. Peebles, N.C. Luhmann, Nucl. Fusion, **27**, 12 (1987)
[5] C. Fenzi, X. Garbet, A. Truc, H. Capes, P. Devynck et al., Nucl. Fusion, **40**, 9 (2000)
[6] S. Sugita, P. Beyer, G. Fuhr et al., Jour. Phys. Society Japan, **81**, 034501, (2012)
[7] J.M. Kwon, S. Yi, T. Rhee et al., Nucl. Fusion, **52**, 013004, (2012)
[8] A. Krämer-Flecken, S. Soldatov, B. Vowinkel et al., Rev. Sci. Instrum. 81, 113502 (2010)
[9] S. Soldatov, A. Krämer-Flecken, O. Zorenko, Rev. Sci. Instrum. 82, 033513 (2011)